Title Page

1   Abrupt permafrost thaw triggers microbial bloom and increased activity of

2   microbial predators

3   Authors

4   Maria Scheel[1], Athanasios Zervas[2], Alexander Tøsdal Tveit[3], Ruud Rijkers[4], Flemming Ekelund[5],

5   Carsten Suhr Jacobsen[2], Torben Røjle Christensen[1,5]

6   Corresponding author

7   Maria Scheel; maria.scheel@ecos.au.dk; +31 618 798369

8   Aarhus University, Frederiksborgvej 399, 4000 Roskilde, Denmark

9

10   Affiliations

11   1   Department of Ecoscience, Aarhus University, Roskilde, Denmark

12   2   Department of Environmental Science, Aarhus University, Roskilde, Denmark

13   3   Department of Arctic and Marine Biology, University of Tromsø, Tromsø, Norway

14   4   Department of Ecological Science, Vrije Universiteit Amsterdam, Amsterdam, The

15   Netherlands

16   5   Department of Biology, Copenhagen University, Copenhagen, Denmark

17   6   Oulanka Research Station, Oulu University, Oulu, Finland

20   **Abstract**

21   Permafrost soils store a substantial part of the global soil carbon, but due to global warming,

22   abrupt erosion and consecutive thaw make these carbon stocks vulnerable to microbial

23   decomposition into greenhouse gases. Although in temperate systems trophic interactions

24   promote soil carbon storage, their role in Arctic permafrost microbiomes, especially during

25   thaw, remains largely unknown. Here, we investigated the microbial response to *in situ* thawing

26   and rapid permafrost erosion. We sequenced the total RNA of a 1 m deep soil core from an

27   active abrupt erosion site to analyse the microbial community in the active layer soil, recently

28   thawed and intact permafrost, consisting of up to 26 500-year-old material. We found

29   maximum RNA:DNA ratios in recently thawed permafrost, indicating upregulation of protein

30   biosynthesis upon thaw. At the same depths, the relative abundance of several prokaryotic

31   orders, including Sphingobacteriales, Burkholderiales, and Nitrosomonadales increased in

32   relative abundance. Bacterial predators were mainly dominated by Myxococcales. Protozoa

33   were overall less abundant but doubled in relative abundance between the active layer and

34   recently thawed permafrost. Cercozoa, Amoebozoa, and Ciliophora were the most abundant

35   protozoan predators, replacing myxobacteria at deeper thaw depths. Overall, connections

36   between the active layer and especially upper thawed layers were visible and suggest

37   migration, while no layer formed a distinct community. Our findings highlight the importance of

38   predation and population dynamics as well as the rapid development of a microbial bloom in

39   abruptly thawing permafrost.

1. Introduction

40

41 Permafrost soils encompass over half of all global soil carbon while harbouring unique but

42 poorly described microbial communities under constant freezing conditions (Hugelius et al.,

43 2014; Tarnocai et al., 2009). Permafrost is ground frozen perennially, for at least two years, and

44 consists of a seasonally thawing active layer, the permanently frozen permafrost, and an

45 interjacent zone of progressing thaw. Additional to gradual thaw, global warming causes

46 ground ice to melt and soils to collapse abruptly, affecting up to half of all permafrost carbon by

47 2100 (Turetsky et al., 2020). Hence, permafrost carbon increasingly becomes available to

48 deeper rooting vegetation and microbial decomposition. However, predictions of future carbon

49 release from permafrost are uncertain due to high spatial variability, but also knowledge gaps

50 related to microbial contributions to fluxes (Elberling et al., 2013; IPCC, 2021).

51 The set of microorganisms, the microbiome, of frozen permafrost differs significantly from

52 overlaying thawed soils. Seasonally fluctuating temperature selects for highly resilient taxa with

53 high growth rates and effective carbon use (Bardgett and Caruso, 2020). In contrast, permafrost

54 - due to stable freezing temperatures - harbours liquid water only in salty brine channels and

55 stores the majority of nutrient-poor carbon as highly recalcitrant organic matter (Parmentier et

56 al., 2017). These conditions select for highly resistant taxa – slow growth rates and higher

57 metabolic versatility (Allison and Martiny, 2008; Shade et al., 2012). While thawed soil

58 communities are often functionally redundant (Nannipieri et al., 2017), permafrost

59 communities have been suggested to be functionally constrained due to environmental

60 limitations and slow reproduction rates (Monteux et al., 2020). Possible microbial responses to

61 thaw include the termination of former resting stages, such as cysts and endospores (Lennon

62   and Jones, 2011), which upon suitable thermal and moisture conditions can lead to local

63   microbial blooms. Alternatively, the active layer microbiome can colonize thawed layers

64   through cryoturbation (Gittel et al., 2014a), active layer detachments (Inglese et al., 2018), or

65   root growth (Monteux et al., 2020). These migrations, or coalescence effects, can increase

66   carbon and nitrogen release from thawed and inoculated permafrost soil (Monteux et al.,

67   2020).

68   Soil microbial biodiversity highly influences the microbiome's resilience toward climate

69   extremes (Bardgett and Van Der Putten, 2014; Griffiths and Philippot, 2013). Furthermore, it

70   has previously been observed that also complexity or quality, and quantity of trophic relations

71   inter- and intrakindom, especially including predation of bacteria (Geisen et al., 2021; Thakur

72   and Geisen, 2019) The decrease of soil biodiversity in temperate systems has been linked to

73   increased losses of carbon to the atmosphere, but within Arctic soil metacommunity, little

74   research has been conducted on this topic.

75   While the role of microbial predators in temperate soils has been studied extensively (Thakur

76   and Geisen, 2019), bacteria-protozoan interactions in thawing permafrost have not been

77   thoroughly explored, although microbial predator presence has been documented (Malard and

78   Pearce, 2018; Scheel et al., 2022; Schostag et al., 2019; Shatilovich et al., 2009). Previous

79   research on thawing permafrost soil has included incubation or gradual thaw gradients, but few

80   microbial studies were conducted on abrupt permafrost erosion sites. However, research has

81   focused on only a few sites extensively, although biogeography of permafrost microorganisms

82   is spatially highly variably, leaving particularly Greenland highly understudied (Malard and

83   Pearce, 2018; Metcalfe et al., 2018). Finally, remote Arctic microbial work is often limited to

84   DNA-based approaches, such as amplicon sequencing, as local processing or transport of RNA is

85   rarely possible. The use of ribosomal RNA (rRNA[1]) community analysis has the clear advantage

86   of decreasing methodological, such as polymerase chain reaction (PCR), biases when utilizing

87   DNA and allowing an understanding of the putatively active community as opposed to

88   metagenomic studies.

89   Here, we overcome these limitations by sampling an *in situ* abrupt erosion site for the first

90   metatranscriptomic analysis of the total active microbial community of Greenlandic permafrost.

91   We hypothesise that the freshly thawed soils support fast-growing species that either invaded

92   from the active layer or consist of reactivated permafrost resting stages. We furthermore test if

93   trophic dynamics impact the community more than abiotic soil properties. These insights can

94   help to understand the spatiotemporal and trophic dynamics of permafrost microbial ecology

95   and estimate the ecological response of warming and rapid erosion as a potential key driver of

96   both permafrost carbon and endemic taxa vulnerability.

---

[1] Abbreviations:
rRNA - ribosomal RNA
mRNA - messenger RNA
PCR - polymerase chain reaction
AL- active layer
TZ - transition zone
PF - permafrost
SOM - soil organic matter
H_2O - soil moisture
AY - young-aged material
AM - medium-aged material
AO - old-aged material
NMDS - non-metric multidimensional scaling
SAR - supergroup Stramenopiles-Alveolata-Rhizaria

2. Materials and Methods

2.1. Soil sampling

Sampling took place within a recent thermal erosion gully situated in Zackenberg valley, NE Greenland (Fig. 1 A-B), as described before (Christensen et al., 2020; Scheel et al., 2022). Below the active layer (AL) at 40 cm depth, an ice lens had melted in 2019, creating a first transition zone depth until 70 cm depth (TZ1) that deepened until 90 cm depth in 2020 (TZ2), while below 90 cm depth intact permafrost (PF) persisted (Fig. 1 C-D). In 2020, we sampled soil down to 100 cm depth aseptically in triplicate per 10 cm horizon. The samples were stored at −20 °C until transported frozen to Denmark, where they were stored at −80 °C.

2.2. Physicochemical soil analysis

Physical soil properties from thawed triplicates per 10 cm were determined as described by Scheel and colleagues (Scheel et al., 2022). In short, weight-based relative soil moisture (H_2O) and organic carbon content (SOM) were calculated by air-drying at 70 °C for 48 h and burning at 450 °C for 2 h. Radiocarbon dating was performed on sieved macrofossils. For the pH measurement, 10 ml of airdried soil were shaken for 1h in 50 ml of 1 M KCl in technical triplicates using a Mettler Toledo FiveEasy PlusTM pH Meter (Mettler Toledo GmbH, Gieben, Germany). The ^{14}C results were split into three age categories for downstream statistical analysis: young soils (AY, until 40 cm depth), medium old soils (AM, 40–60 cm depth ranging from 2 645 to 3 770 years BP), and old soil (AO, from 60 cm depth and below with up to 26 500–year-old material Table 1).

6

117   *Table 1 Soil properties include ^{14}C radiocarbon dating results (* = fM; **BP), relative weight-based soil moisture (H_2O), relative*

118   *weight-based soil organic matter content (SOM), pH and layer, as defined by thawing processes as active layer (AL), deepest*

119   *thaw in 2019: transition zone 1 (TZ1) and 2020: TZ2; and permafrost (PF). Extraction and sequencing output included the*

120   *calculated RNA:DNA ratio based on co-extraction of nucleic acids per gram dry weight (gDW). The cumulative sum of clean total*

121   *RNA sequencing reads per depth. Standard deviations for triplicates per depth are indicated where available (±).*

depth [cm]	^{14}C [*fM **BP]	H_2O [%]	SOM [%]	pH	layer	DNA gDW [ng/µl]	RNA gDW [ng/µl]	RNA:DNA	total reads
0-10	1.04*	28.80 ± 3.38	8.73 ± 1.82	4.22 ± 0.03	AL	16.70 ± 7.84	7.15 ± 3.43	2.34 ± 0.43	1.78E+07
10-20	1.13*	22.52 ± 0.73	5.39 ± 0.83	4.02 ± 0.05		1.65 ± 1.86	1.46 ± 0.17	1.11 ± 0.90	4.85E+07
20-30	1.16*	22.05 ± 3.30	10.19 ± 3.22	4.29 ± 0.01		11.23 ± 11.43	1.82 ± 0.04	6.11 ± 0.16	2.25E+07
30-40	1.2*	26.57 ± 0.83	13.68 ± 0.44	4.25 ± 0.01		3.73 ± 0.67	1.73 ± 0.46	2.18 ± 0.46	1.05E+08
40-50	2 635**	7.73 ± 1.58	2.59 ± 0.68	4.63 ± 0.03	TZ1	1.09 ± 1.20	0.81 ± 0.85	1.37 ± 0.73	2.39E+07
50-60	3 770**	15.61 ± 6.28	2.93 ± 0.30	4.13 ± 0.02		0.22 ± 0.19	0.81 ± 0.21	0.27 ± 3.75	7.22E+07
60-70	26 500**	8.72 ± 2.53	1.52 ± 0.16	4.86 ± 0.05		0.17 ± 0.23	0.72 ± 0.09	0.23 ± 4.43	4.90E+07
70-80	22 100**	6.35 ± 0.60	1.10 ± 0.24	4.48 ± 0	TZ2	0.04 ± 0.04	0.36 ± 0.62	0.11 ± 9.13	1.49E+07
80-90	26 200**	7.96 ± 0.61	1.00 ± 0.20	4.57 ± 0.01		0.02 ± 0.04	NA	NA	3.46E+07
90-100	26 200**	7.80 ± 0.59	1.04 ± 0.26	4.91 ± 0.01	PF	0.02 ± 0.03	NA	NA	1.40E+07

122

123   2.3.   **Nucleic acid co-extraction, library preparation, and sequencing**

124   We homogenised the flash-frozen samples in antiseptic mortars before co-extracting the total

125   RNA and DNA of the biological replicates on up to 0.35 g frozen soil sample in technical

126   triplicate with the NucleoBond RNA Soil Mini kit (Macherey-Nagel GmbH & Co. KG Dueren,

127   Germany) according to the manufacturer's protocol, but including added G2 DNA/RNA

128   Enhancer infused 1,4 mm beads (Ampliqon, Odense, Denmark). Resulting concentrations were

129   normalised for the sample weight and used for extraction ratios of extracted RNA to DNA

130   (RNA:DNA). The RNA was further DNase-treated, cDNA synthesised, and metabarcoded as

131   described by Mondini and colleagues (Mondini et al., 2022). All purification and library

132   preparation steps were executed in a dedicated PCR clean room and for all nucleic acid

133   concentrations evaluated with the TapeStation 4150 (Agilent Technologies, Santa Clara,

134   California, US). RIN values were low (1.0 ± 0.6, SI Table 1); hence the samples were pooled into

135   equimolar libraries to secure even sequencing coverage and were sequenced in-house

136   (Department of Environmental Sciences, Aarhus University, Denmark) on a NextSeq 500 with a

137   v2.5 high-throughput 300 cycles kit (both Illumina, San Diego, CA, United States).

138   2.4.   **Quality filtering, RNA sorting, and OTU mapping**

139   Raw paired-end Illumina reads (SRA accession number: PRJNA853791) were quality-controlled

140   with TrimGalore (https://www.bioinformatics.babraham.ac.uk/projects/trim_galore/) and then

141   sorted into small subunit (SSU) rRNA and non-rRNA bins using SortMeRNA (Kopylova et al.,

142   2012). The SSU reads were assembled into full-length SSU rRNA contigs with MetaRib (Xue et

143   al., 2020). These contigs were taxonomically classified as described by Anwar and colleagues

144   (Anwar et al., 2019), using CREST (Lanzén et al., 2012) against the SILVA database v. 128 (Quast

8

145 et al., 2013), resulting in taxonomically annotated rRNA contigs abundance across 30 sample

146 triplicates. The resulting taxonomy was utilised throughout this work.

147   2.5.   **Community analysis and statistical testing**

148 We performed community analysis with the R software in the R studio environment (R Core

149 Team, 2021; R Studio Team, 2021), utilising the phyloseq (McMurdie and Holmes, 2013) and

150 vegan packages (Oksanen et al., 2020). Shannon (S) alpha diversity and richness (number of

151 rRNA contigs) per sample were calculated. The significance of environmental data (^{14}C-age, pH,

152 SOM, H_2O, and layer) was tested with the *anova* function (*PERMANOVA*, 999 permutations) on

153 Bray-Curtis dissimilarities of relative abundance per taxa within the sample to account for

154 different read coverage across samples. Consecutive Tukey's HSD post hoc tests were

155 performed. Principal component analyses and non-metric multidimensional scaling (NMDS)

156 were ordinated graphically using Bray-Curtis dissimilarities. The total community was scanned

157 for previously documented eukaryotic and bacterial predators (Geisen et al., 2015; Petters et

158 al., 2021).

159 ## 3. Results

160   3.1.   **Sequencing success and overall community composition**

161 Extraction of RNA and DNA was successful in all triplicates and RNA:DNA ratios indicated higher

162 values in the transition zones (Fig. 2, SI Table 1). Overall, we obtained 49 million clean paired-

163 end Illumina reads. In total, 1952 full-length gene rRNA contigs were constructed with an

164 average length of 1475 bp. Annotation was complete on domain level but decreased above

165 class level (SI Table 1). On average, 72.9% of all reads could be annotated as SSU rRNA reads

166   and 62.3% of the raw reads mapped against these. Overall, 1833 rRNA contigs were assigned as

167   Bacteria, 109 rRNA contigs as Eukarya, and nine rRNA contigs as Archaea.

168   3.2.   **Prokaryotic community composition and distribution with depth**

169   The prokaryotic community was dominated by Proteobacteria (31.4 ± 9.6% of total counts),

170   Actinobacteria (15.8 ± 7.1% of total counts), Acidobacteria (8.6 ± 5.3% of total counts),

171   Chloroflexi (6.4 ± 4.1% of total counts) and Planctomycetes (5.4 ± 2.9% of total counts, Fig. 3A).

172   Additional 28 bacterial and five archaeal phyla were present and included three methanogenic

173   rRNA contigs (0.03 ± 0.01% of total counts) and eight methanotrophic rRNA contigs (0.61 ±

174   0.11% of total counts). Proteobacteria were dominated by Betaproteobacteria (15.3 ± 12.7% of

175   total counts) and therein by the Nitrosomonadales (6.2 ± 6.6% of total counts) and

176   Burkholderiales order (5.1 ± 5.0% of total counts), with maximum abundances at 70 cm and 90

177   cm depth, respectively. Deltaproteobacteria (8.2 ± 5.3% of total counts) decreased with depth

178   from 50 cm depth on, mainly controlled by Myxococcales abundances (6.4 ± 4.7% of total

179   counts). Alphaproteobacteria (6.6 ± 2.3% of total counts), especially the Rhizobiales order (4.5 ±

180   1.6% of total counts), were abundant both at the surface and permafrost. Actinobacteria

181   abundance decreased between 40–80 cm and reached a maximum at 90–100 cm. At the latter

182   depth, Chitinophagia and Cytophagia were abundant, with *Cytophaga aurantiaca* as the most

183   abundant contig, mapping 5.0 ± 4.0% of all permafrost counts. Bacteroidetes abundance

184   increased with depth, reaching a maximum at 70–80 cm, particularly driven by one

185   Sphingobacteriales contig, which alone constituted 13.3 ± 9.3% of all counts at this depth.

186   While 980 contigs (30% of total counts) were more abundant in AL than in deeper samples, 200

187   of these, mainly Acidobacteria, Planctomycetes, Chloroflexi, and Myxococcales contigs, were

188   also abundant in the first transition zone, accounting together for 7.5% of all counts. In

189   contrast, 158 contigs were exclusively (over 90%) abundant in the active layer, including several

190   Planctomycetes, Acidobacteria, and Chloroflexi contigs.

191   In the transition zones, 659 contigs (53% of total counts) were more abundant than in other

192   layers, typified by the Nitrosomonadales and Burkholderiales orders, as well as Cercozoa and

193   Ciliophora contigs. Particularly, 100 contigs (9% of total counts) were more abundant in TZ2

194   than in any other layer, including many Sphingobacteriales contigs. Of these, 28 contigs were

195   more abundant in permafrost than in TZ1, of which 11 consisted of Burkholderiales contigs.

11

Table 2 Average relative abundances in % per total prokaryotic community including prokaryotes (prok; *excluding prokaryotic predators) and their predators (= pred) per depth

horizon. These include all predatory taxa (pred), in particular the bacterial predatory (bacpred) orders Bdellovibrionales and Myxococcales, as well as eukaryotic protozoan

superkingdoms (prot). Standard deviation is given in ±, accounting for the triplicates per depth.

depth [cm]	0-10	10-20	20-30	30-40	40-50	50-60	60-70	70-80	80-90	90-100
prok*	68.40 ± 1.75	88.36 ± 0.84	85.27 ± 1.03	76.26 ± 1.18	70.66 ± 2.76	73.84 ± 5.63	75.76 ± 4.19	77.89 ± 1.43	74.74 ± 3.43	81.76 ± 3.03
total pred	10.91 ± 0.67	6.85 ± 0.20	9.36 ± 0.04	16.94 ± 0.42	17.59 ± 2.76	13.83 ± 4.25	11.65 ± 1.88	7.78 ± 0.69	6.26 ± 0.30	6.06 ± 1.80
bacpred	7.29 ± 0.74	5.20 ± 0.20	7.19 ± 0.03	13.71 ± 0.25	11.46 ± 3.37	7.97 ± 6.60	4.35 ± 1.78	2.14 ± 0.53	1.06 ± 0.13	2.18 ± 2.27
Bdellovibrionales	0.14 ± 0.01	0.11 ± 0.02	0.15 ± 0.01	0.22 ± 0.01	0.33 ± 0.09	0.27 ± 0.13	0.41 ± 0.07	0.49 ± 0.02	0.28 ± 0.07	0.16 ± 0.17
Myxococcales	7.15 ± 0.73	5.09 ± 0.19	7.04 ± 0.04	13.49 ± 0.26	11.14 ± 3.30	7.70 ± 6.55	3.94 ± 1.71	1.65 ± 0.52	0.78 ± 0.11	2.02 ± 2.10
Haliangium	2.67 ± 0.41	1.69 ± 0.02	2.57 ± 0.24	5.81 ± 0.45	6.07 ± 2.89	4.65 ± 5.24	1.24 ± 0.60	0.40 ± 0.18	0.11 ± 0.01	0.66 ± 0.85
Polyangium	1.07 ± 0.08	0.59 ± 0.07	0.51 ± 0.01	1.19 ± 0.08	0.65 ± 0.08	0.37 ± 0.21	0.39 ± 0.16	0.34 ± 0.34	0.22 ± 0.03	0.34 ± 0.17
protozoa	3.62 ± 0.60	1.65 ± 0.21	2.17 ± 0.04	3.23 ± 0.59	6.13 ± 2.15	5.85 ± 1.89	7.31 ± 1.98	5.64 ± 0.84	5.19 ± 0.47	3.88 ± 1.33
Amoebozoa	1.16 ± 0.21	0.55 ± 0.04	0.67 ± 0.02	0.82 ± 0.17	1.06 ± 0.34	1.16 ± 0.52	1.09 ± 0.43	0.48 ± 0.15	0.47 ± 0.08	0.33 ± 0.40
Excavata	0.34 ± 0.04	0.24 ± 0.05	0.26 ± 0.03	0.49 ± 0.10	0.59 ± 0.31	0.50 ± 0.06	0.83 ± 0.20	0.69 ± 0.28	0.54 ± 0.23	0.38 ± 0.22
Choanoflagellata	0.13 ± 0.02	0.04 ± 0.01	0.07 ± 0.02	0.11 ± 0.03	0.17 ± 0.08	0.11 ± 0.05	0.12 ± 0.04	0.12 ± 0.05	0.08 ± 0.03	0.05 ± 0.07
SAR	2.34 ± 0.42	1.12 ± 0.06	1.49 ± 0.02	2.38 ± 0.40	6.89 ± 1.14	6.66 ± 2.21	7.42 ± 3.02	7.09 ± 0.35	7.32 ± 0.42	4.96 ± 0.64
Cercozoa	1.27 ± 0.12	0.76 ± 0.10	0.76 ± 0.06	1.21 ± 0.20	2.96 ± 1.18	2.80 ± 0.91	3.48 ± 1.07	2.66 ± 0.51	2.50 ± 0.11	2.09 ± 0.38
Ciliophora	0.60 ± 0.13	0.13 ± 0.05	0.44 ± 0.05	0.57 ± 0.14	1.18 ± 0.24	0.98 ± 0.51	1.52 ± 0.68	1.34 ± 0.19	1.34 ± 0.13	0.71 ± 0.20
Stramenopiles	0.10 ± 0.02	0.05 ± 0.01	0.05 ± 0.00	0.13 ± 0.02	0.23 ± 0.06	0.36 ± 0.10	0.28 ± 0.05	0.38 ± 0.26	0.31 ± 0.09	0.31 ± 0.10
Hacrobia	0.03 ± 0.00	0.01 ± 0.00	0.01 ± 0.00	0.02 ± 0.00	0.03 ± 0.01	0.03 ± 0.02	0.05 ± 0.03	0.03 ± 0.01	0.03 ± 0.01	0.01 ± 0.02
pred:prok	0.15 ± 0.02	0.08 ± 0.01	0.11 ± 0.00	0.22 ± 0.01	0.24 ± 0.08	0.19 ± 0.13	0.15 ± 0.06	0.10 ± 0.00	0.08 ± 0.01	0.07 ± 0.05
prot:bacpred	0.50 ± 0.03	0.32 ± 0.03	0.30 ± 0.01	0.24 ± 0.05	0.55 ± 0.15	0.99 ± 0.53	1.76 ± 0.36	2.80 ± 1.00	4.91 ± 0.46	2.97 ± 1.80

199

3.3. Non-predatory Eukarya

Within the Archaeplastida (6.5 ± 2.9% of total counts), the most abundant phylum was Tracheophyta (5.6 ± 2.4% of total counts) accounting for 38.5% of all eukaryotic counts, dominated by Magnoliophyta rRNA contigs. The supergroup Stramenopiles-Alveolata-Rhizaria (SAR) contigs (4.8 ± 2.8% of total counts) on average made up 33.6% of all eukaryotic counts, increasing in the transition zones. Opisthokonta (1.5 ± 2.1% of total counts) abundance included Fungi, particularly Ascomycota and Basidiomycota, and Metazoa mainly at 0–10 cm and decreased with depth (Fig. 3C).

3.4. Bacterial and eukaryotic bacterivores abundance

Bacterivores included bacterial predators of the Deltaproteobacteria class, as well as several protozoan taxa (Fig. 3B, Table 2, for all taxonomic annotations see SI. Table 2). Myxococcales was the overall most abundant order and dominated the 140 bacterial predator rRNA contigs (6.0 ± 4.5% of total counts), with *Haliangium* and *Polyangium* as the most abundant genera. Especially *Haliangium* dominated (2.6 ± 2.7% of total counts) the boundary between the active layer and thawed permafrost at 40–50 cm depth.

The microeukaryotic protozoa included 72 rRNA contigs (4.5 ± 2.1% of total counts). Cercozoa (2.1 ± 1.1%) and Ciliophora (0.9 ± 0.5%) were most abundant throughout both transition zones and reached a maximum at 60–70 cm depth (together 5 ± 1.8% of total counts). Amoebozoa (0.9 ± 0.4%), especially Lobosa contigs, were most abundant at the top 0–10 cm sample and in TZ1 (Fig. 3D). We tested whether relative abundances of selected prokaryotic taxa and predator contig correlated (SI Fig. 1) but found no significant correlation.

13

3.5. Diversity, ordination, and drivers of trends (ANOSIM)

Shannon alpha diversity reached a maximum at 40 cm depth, with an average 6.21 ± 0.18 for all domains, and decreased with depth below 40 cm (Fig. 4). Protozoan richness reached 72 rRNA contigs at all depths, while 140 bacterial predator rRNA contigs occurred in 28 of 30 triplicates.

Principal Component Analysis revealed a clear grouping of the AL samples versus deeper samples, explaining 43.5 ± 2.5% of variation on the first axis per tested group (prokaryotes, eukaryotes, bacterial and eukaryotic predators; Fig. 5, NMDS see SI Fig. 2). ANOVA results confirmed this trend with layer explaining most of the variation in the dataset (F.Model = 6.09, R^2 = 0.75, p = 0.002; Table 3). Except for pH (F.Model = 2.66, R^2 = 0.25, p = 0.054), age (F.Model = 5.07, R^2 = 0.59, p = 0.002), SOM (F.Model = 5.01, R^2 = 0.39, p = 0.001) and H_2O (F.Model = 5.26, R^2 = 0.4, p = 0.009) were found significant to explain community dissimilarities. Tukey's HSD tests revealed no significant differences between communities along layer or age categories, except a significant difference between AL and PF samples in the total (adjusted p = 0.048), prokaryote (adjusted p = 0.048) and protozoan (adjusted p = 0.042) community dissimilarities. When we tested, if predator relative abundance significantly shapes the total community, we found that Protozoa most significantly shaped the prokaryotic (F.Model = 3.86, R^2 = 0.33, p = 0.015), as well as the bacterial predator community (F.Model = 5.65, R^2 = 0.41, p = 0.017). Meanwhile, bacterial predators had slightly less impact on the prokaryotic (F.Model = 3.34, R^2 = 0.29, p = 0.03) and protozoan community (F.Model = 3.19, R^2 = 0.29, p = 0.039).

14

240 *Table 3 ANOVA statistical analysis on mean Bray-Curtis dissimilarities per depths between total community, prokaryotic (prok; *excluding prokaryotic predators), bacterial*

241 *predators (bacpred), eukaryotic and protozoan (prot) rRNA contigs. These were tested against the environmental parameters of age (14C), layer, soil organic matter (SOM) and*

242 *moisture (H_2O), pH and the presence of non-predatory (*) prokaryotes, bacpred and protozoa per depth. The output includes the F-Model values (F), R2 and P-values (P) < 0.05*

243 *were considered significant and are marked in bold.*

env. Parameter	total			prok			bacpred			eukaryotes			prot		
	F	R^2	P	F	R^2	P	F	R^2	P	F	R^2	P	F	R^2	P
^{14}C	5.069	0.592	**0.001**	5.069	0.592	**0.001**	6.285	0.642	**0.006**	6.906	0.664	**0.004**	6.678	0.656	**0.002**
layer	6.088	0.753	**0.002**	6.088	0.753	**0.001**	5.002	0.714	**0.006**	6.008	0.750	**0.003**	6.881	0.775	**0.001**
SOM	5.010	0.385	**0.004**	5.010	0.385	**0.004**	6.924	0.464	**0.009**	6.389	0.444	**0.005**	6.072	0.432	**0.006**
H_2O	5.260	0.397	**0.009**	5.260	0.397	**0.005**	5.691	0.416	**0.014**	7.240	0.475	**0.007**	7.242	0.475	**0.008**
pH	2.655	0.249	0.054	2.655	0.249	0.059	3.430	0.300	0.057	2.803	0.259	0.065	2.897	0.266	0.059
prok*	-	-	-	-	-	-	1.645	0.171	0.180	0.880	0.099	0.405	1.057	0.117	0.336
bacpred	-	-	-	3.336	0.294	**0.030**	-	-	-	3.771	0.320	**0.032**	3.190	0.285	**0.039**
prot	-	-	-	3.857	0.325	**0.015**	5.648	0.414	**0.017**	4.284	0.349	**0.024**	-	-	-

244

15

4. Discussion

4.1. RNA:DNA ratio indicates active bloom

The use of total RNA sequencing, such as metatranscriptomics, enables the description of the entire soil community with full-length rRNA sequencing, including prokaryotic and eukaryotic taxa. Especially the relative abundance of Eukarya is often underestimated or removed from metatranscriptomic datasets, but few studies formerly confirmed similar results as in this work with 10% (Tveit et al., 2013; Urich et al., 2008), while another relevant study only found 0.07% fungi as eukaryotes (Hultman et al., 2015). The eukaryotic alpha diversity was similar to former metatranscriptomic permafrost studies (Tveit et al., 2015), or even higher (Hultman et al., 2015), and the overall low fungal abundances could relate to the rapid decrease of fungi upon thaw, as shown before (Schostag et al., 2019). Meanwhile, the co-extraction of DNA also supplies RNA:DNA ratios to infer the overall activity: the total extracted RNA consists mainly of ribosomal RNA, of which ribosomes are responsible for translating messenger (mRNA) into proteins for cell growth. Our findings of higher RNA:DNA ratios at the freshly thawed 50 and 80 cm depth hence indicate a relatively higher ribosomal abundance at these depths. To understand, which taxa are the most active, we here explore fast-growing prokaryotes and all microbial predator abundances.

4.2. Dominant prokaryotes in thawing permafrost soil

Overall, Proteobacteria contigs were the most abundant and encompassed the most phylogenetically and metabolically diverse groups. Especially Betaproteobacteria responded strongly to thaw, in line with their formerly documented copiotrophic representatives, responding quickly to freshly available resources (Hurst, 2019; Schostag et al., 2019).

16

267   Particularly Nitrosomonadales occurred at the first erosion year's maximum thaw depth of 70

268   cm. Schostag and colleagues showed that the Nitrosomonadaceae relative abundance

269   correlated with nitrogen pools in permafrost soils (Schostag et al., 2019). Here, especially the

270   family Gallionellaceae contains nitrate-dependent ferrous iron-oxidising taxa (He et al., 2016)

271   and was previously found in partly ancient permafrost (Alawi et al., 2007; Müller et al., 2018;

272   Scheel et al., 2022). Notably, most genera with maximum relative abundances at this depth (70

273   cm), were putative ammonia oxidizers within Betaproteobacteria. Many of these are

274   conditionally rare, but metabolically important taxa, as they can respond rapidly to changing

275   environmental factors (Shade et al., 2014). Although nutrient measurements and nitrification

276   gene abundance are needed to confirm active gene expression, our results confirm the

277   ecological importance of nitrogen cycling in thawing permafrost, as suggested before (Keuper

278   et al., 2020; Monteux et al., 2020). Among the Betaproteobacteria, Burkholderiales increased

279   steadily towards the second, deepest thaw depth. Most represented by Comamonadaceae, a

280   family that consists of many copiotrophic spore formers, rapidly responding to fresh input of

281   labile nutrients (Fierer et al., 2007; Ho et al., 2017). This suggests that mineral-weathering

282   Burkholderiales (Naylor et al., 2022) are readily responsive to thawing soil conditions. Similarly,

283   the active Bacteroidetes order Sphingobacteriales dominated recently thawed permafrost. In

284   our study site, this order formerly had the highest relative amplicon-based abundance with

285   more than 50% of all counts between 70–90 cm depth in 2020, despite very low abundances

286   one year earlier (Scheel et al., 2022). This confirms that this taxon as a major component of the

287   microbial community at thawed depths, which responds strongly to thaw (Burkert et al., 2019;

17

288   Coolen and Orsi, 2015; Deng et al., 2015; Frank-Fahle et al., 2014) and is abundant at the upper

289   permafrost limit (Müller et al., 2018; Tripathi et al., 2018).

290   The large taxonomic shifts in the rRNA pool suggest that the ancient carbon that became

291   available due to warmer temperatures at these depths allows decomposers to thrive. Former

292   studies have shown that methane emissions from this site were variable in both space and time

293   during collapse (Scheller et al., 2021), which highlights the potential of a biogenic carbon

294   release.

295   ### 4.3. Thaw layers as strongest abiotic drivers

296   Our results suggest that while edaphic parameters govern the community, based on age and

297   layer as well as soil moisture, pH did not, which could be due to the very small variation in pH in

298   our study. The active layer contained the highest alpha diversity, where a distinct community

299   had formed over numerous years, in agreement with former findings (Ganzert et al., 2014;

300   Gittel et al., 2014a; Monteux et al., 2018). Many microbial taxa, especially within the predator

301   community, responded rapidly to thaw, after the former ice lens as separation between the

302   active layer and deeper soils thawed. This could enable dispersal into deeper soils, although we

303   expect this to be an overall slow process as we expect an overall still low soil temperature and

304   nutrient availability. An amplicon-based study at this site still confirmed similar emerging

305   drivers, mainly layer and age (Scheel et al., 2022), as the only soil microbial studies performed

306   locally before (Ganzert et al., 2014; Gittel et al., 2014b). Overall, more than half of all counts

307   stem from taxa dominantly present in the thawed layers. Yet, no significant differences were

308   found between the two thawed layers, which suggests that the thawed layers form a gradient

309   between the significantly distinct historic active layer and permafrost communities, rather than

18

310   giving rise to a differentiated biome. Although age was as significantly explaining the variance in

311   total community dissimilarities as the layers, we hypothesize that this is due to the complete

312   active layer being of younger age and that those dissimilarities are mainly driven by the

313   different active layer community compared with the rest. As we did not detect significant

314   differences between the age categories, we assume that community changes rather took place

315   across both selected depths within the oldest layers, where the most recent thaw took place.

316   It has been discussed how the thermal state of permafrost depicts clear dispersal limits for

317   water-dependent species such as most prokaryotic taxa. We argue this to be true for the

318   similarly significant impact of soil moisture on the community at the moment of sampling.

319   These edaphic properties depict the rather short-term character of the site. Especially fast-

320   growing species adapt quickly to changing ecosystem parameters, due to their small size and

321   high doubling times. We hypothesize, that this could explain the high RNA content we

322   particularly found in the thawed permafrost material of the rapidly thawing soils, where several

323   taxa quickly adapt to the more suitable conditions of available water and warmer

324   temperatures.

4.4.   Predation patterns as a response to thaw dynamics

326   We found bacterivores to be among the putatively active community, also within ancient

327   thawing permafrost. Here, the increase of protozoa relative to bacterial predator abundance

328   with recent thaw is largely controlled by the relative increase of protozoan biomass in formerly

329   less inhabited permafrost layers, where myxobacterial abundances did not increase yet.

330   Whether protozoa in these depths were more mobile or originated from resting stages, is not

331   known, but amplicon-based sequencing at this site confirmed the increase of Myxococcales at

19

332   the 40–50 cm deep first fresh thaw horizon from 2019 to 2020, the year of sampling for this

333   study. While this trend could stem from preserved rRNA, although possibly not stable for longer

334   than several weeks in thawed soil (Schostag et al., 2020), we do not find the same level of

335   preservation for both kingdoms of predators, indicating a truly active microeukaryotic bloom

336   with permafrost thaw. Our *in situ* approach gives rise to the idea of more mobile predators

337   dominating during the initial stages of the thaw-triggered microbial bloom, while consecutive

338   migration of bacterial predators in later stages of thaw could be possible as well. This shows

339   that abrupt thaw triggers the microeukaryotic community, suggesting an important role of

340   eukaryotic predators during the initial stages after thaw and thus substantially expanding on

341   previous studies of Schostag and colleagues, who found an increased abundance of

342   microeukaryotes during controlled short-term thaw (Schostag et al., 2019).

4.4.1.   *Bacterial predators from the active layer*

344   We found that Myxococcales was the overall most dominant taxonomic order, especially at the

345   interface between the active layer and transition zone. Myxococcales are highly abundant in

346   Arctic soils (Malard and Pearce, 2018), and have been observed at this study site before (Scheel

347   et al., 2022). Bacterial predators and particularly Myxococcales may play key roles in microbial

348   food webs, as recently demonstrated (Dai et al., 2021; Petters et al., 2021). Within the active

349   layer, seasonal prokaryotic blooms support higher prey and predator abundance and we

350   hypothesize that the formation of spore-containing fruiting bodies in Myxococcales (Huntley et

351   al., 2011) offers resistance to the winter freeze-off. In contrast, Bdellovibrionales were found at

352   a deeper thaw depth, which might indicate a higher mobility within the soil profile, based on

20

353   their flagellate morphology and the significant impact of soil moisture on migration (Petters et

354   al., 2021).

355   Bacterial predator abundance explained less variation in the beta diversity of prokaryote

356   abundances than protozoa, which might due to the significantly higher protozoan abundances

357   within the microbial bloom in the transition zone. Furthermore, Myxobacteria were found to

358   select on gram-negative bacteria, while protozoa showed less selective feeding, hence

359   benefiting from gram-positive bacteria (Zhang and Lueders, 2017), which in our samples were

360   especially abundant in thawed depths, including Bacilli and Clostridia, e.g., with Clostridia also

361   an abundant spore former in ancient permafrost (Johnson et al., 2007).

362   4.4.2. *Protozoa as fast responding predators*

363   Eukaryotic predators included Cercozoa, Amoebozoa, and Ciliophora in agreement with the few

364   former studies (Schostag et al., 2019; Shatilovich et al., 2009). Members of the eukaryotic

365   predator community responded similarly to permafrost thaw, as Ciliophora and Cercozoa

366   reached maximum abundances at 70 cm depth, responding to the deepest thaw depths in the

367   first erosion year. Interestingly, we expected higher abundances of relatively smaller Cercozoa

368   due to their smaller size and hence faster doubling times (Rønn et al., 2012) at the most

369   recently available thaw horizon at 90 cm. They have been documented to respond quickly to

370   thaw in a matter of days (Schostag et al., 2019), while they were also seen to respond rapidly to

371   temperature increases (Tveit et al., 2015). Our findings match these observations with Cercozoa

372   contributing to more than 2% of total abundance per sample, they dominate the protozoan

373   bloom in thawed layers.

21

374 Ciliates and Amoebozoa have been observed in Siberian permafrost previously (Shatilovich et

375 al., 2009). Particularly, the ciliates highly abundant in both transition zones, Spirotrichea and

376 Oligohymenophorea, were also formerly found in ice caves, indicating possible cold adaptation

377 (Mondini et al., 2022). One potential explanation for the high abundance of protozoa in freshly

378 thawed permafrost could be that several cyst- and resting-stage-forming protist taxa have

379 previously responded quickly to environmental changes (Rønn et al., 2012).

380 **4.3. Microbial bloom in thawing soils potentially impacted by coalescence**

381 A microbial bloom, as indicated by large increases in the RNA:DNA ratio acted as the fundament

382 for a larger and more active microbial food web dominated by protozoan bacterivores in soil

383 that thawed recently and bacterial predators in soil that thawed one year ago.

384 Our findings suggest differently timed responses to permafrost thaw could indicate relatively

385 slow and steady progression of active layer taxa into thawed layers, as well as rapid microbial

386 blooms at just thawed former permafrost layers and stress the non-linear and complex

387 ecological response of environmentally stressed soil microbiomes in this setting. These results

388 support our hypothesis, that thawed soils can experience a microbial bloom, consisting of

389 predominantly fast-growing taxa. Our study additionally supports earlier findings that show the

390 potential for coalescence, or migration of the active layer into thawed permafrost communities

391 upon transplantation of surface soil microbiome to permafrost (Monteux et al., 2020). Although

392 we could not statistically separate the potential effects of isolated permafrost thaw and

393 coalescence with the active layer community, we hypothesize that these processes both play a

394 role in the thaw zone, as thawed permafrost communities were indistinguishable from both the

395   permafrost and active layer. In their previous incubation study, Monteux and colleagues could

396   identify abundance changes purely related to thaw, including an increase of Bacteroidetes

397   abundance, apart from coalescence effects stemming from the inoculating soil material

398   (Monteux et al., 2020). In both cases, the processes of thaw and migration have resulted in

399   elevated emissions of greenhouse gases (Monteux et al., 2020), highlighting the importance of

400   understanding community dynamics in response to thaw. Permafrost carbon and nitrogen

401   retention thereby is steered more by community composition than microbial biomass

402   and edaphic properties.

403   ### 4.5.   Conclusion

404   We have demonstrated microbial responses to abruptly eroding permafrost in Greenland and

405   described shifts in the total community and their abiotic and trophic drivers. The novelty of this

406   work includes both one of the rare *in situ* total active community descriptions in intact and

407   eroding permafrost and highlighting the role of predators in response to a microbial bloom

408   during abruptly thawing of ancient permafrost soil horizons. We found evidence for our

409   hypothesis that the freshly thawed transition zones are dominated by fast-growing taxa, as

410   Nitrosomonadales, Sphingobacteriales, and Burkholderiales were dominant in these depths.

411   We see the potential for coalescence as the main driver of the shallow thawed samples, while a

412   bloom of taxa from permafrost could indicate an additional process. To further explore these

413   questions, we recommend stable isotope probing studies that elucidate the origin and

414   dynamics of fast-responding taxa. On top, we suggest a coupling of sequencing and cultivation

415   studies to quantitatively correlate dominant organism abundances, physiology, trophic

416   relations, and carbon and nitrogen cycling capacities. Finally, nestedness analysis could further

417 elucidate these opposing dynamics as well as their effect on the ecosystem functioning in

418 vulnerable but abruptly thawing permafrost environments. While total RNA sequencing might

419 remain challenging in remote environments, metagenomic and mRNA-based approaches need

420 to be incorporated into *in situ* studies from multiple geographic locations, to fully link microbial

421 activity to taxonomic insights. Furthermore, we stress the importance of the described

422 predation patterns, as trophic complexities within microbial soil ecosystems highly impact the

423 total stock vulnerability and resilience to further climatic perturbation.

5. Acknowledgements

6. Competing interests

430 The authors declare no competing financial interests.

7. Data availability statement

432 The raw sequence data of this study were deposited in the NCBI Sequence Read Archive and

433 can be accessed through accession number PRJNA853791.

8. References

435 Alawi, M., Lipski, A., Sanders, T., Pfeiffer, E.-M., Spieck, E., 2007. Cultivation of a novel cold-

436   adapted nitrite oxidizing betaproteobacterium from the Siberian Arctic. ISME J. 256–264.

437   https://doi.org/10.1038/ismej.2007.34

438   Allison, S.D., Martiny, J.B.H., 2008. Resistance, resilience, and redundancy in microbial

439   communities. Proc. Natl. Acad. Sci. U. S. A. 105, 11512–11519.

440   https://doi.org/10.1073/pnas.0801925105

441   Anwar, M.Z., Lanzen, A., Bang-Andreasen, T., Jacobsen, C.S., 2019. To assemble or not to

442   resemble—A validated Comparative Metatranscriptomics Workflow (CoMW). Gigascience

443   8, 1–10. https://doi.org/10.1093/gigascience/giz096

444   Bardgett, R.D., Caruso, T., 2020. Soil microbial community responses to climate extremes:

445   Resistance, resilience and transitions to alternative states. Philos. Trans. R. Soc. B Biol. Sci.

446   375. https://doi.org/10.1098/rstb.2019.0112

447   Bardgett, R.D., Van Der Putten, W.H., 2014. Belowground biodiversity and ecosystem

448   functioning. Nature 515, 505–511. https://doi.org/10.1038/nature13855

449   Burkert, A., Douglas, T.A., Waldrop, M.P., Mackelprang, R., 2019. Changes in the Active, Dead,

450   and Dormant Microbial Community Structure across a Pleistocene Permafrost

451   Chronosequence. Appl. Environ. Microbiol. 85, 1–16.

452   https://doi.org/https://doi.org/10.1128/AEM .02646-18

453   Christensen, T.R., Lund, M., Skov, K., Abermann, J., Scheller, J., Scheel, M., Lo, E., Langley, K.,

454   Murphy, M.J., Mastepanov, M., López-Blanco, E., Scheller, J., Scheel, M., Jackowicz-

455   Korczynski, M., Langley, K., Murphy, M.J., Mastepanov, M., Lo, E., Langley, K., Murphy,

456   M.J., Mastepanov, M., 2020. Multiple Ecosystem Effects of Extreme Weather Events in the

457   Arctic. Ecosystems. https://doi.org/10.1007/s10021-020-00507-6

458   Coolen, M.J.L., Orsi, W.D., 2015. The transcriptional response of microbial communities in

459   thawing Alaskan permafrost soils. Front. Microbiol. 6, 1–14.

460   https://doi.org/10.3389/fmicb.2015.00197

461 Dai, W., Wang, N., Wang, W., Ye, X., Cui, Z., Wang, J., Yao, D., Dong, Y., Wang, H., 2021.

462   Community Profile and Drivers of Predatory Myxobacteria under Different Compost

463   Manures. Microorganisms 9, 1–15.

464 Deng, J., GU, Y., Zhang, J.I., XUE, K., Qin, Y., Yuan, M., YIN, H., ZHILI HE, Wu, L., Schuur, E.A.G.G.,

465   Tiedje, J.M., ZHOU, J., He, Z., Wu, L., Schuur, E.A.G.G., Tiedje, J.M., ZHOU, J., Lansing, E.,

466   Division, S., Berkeley, L., Control, P., Yungfu, G., Zhang, J.I., Xu, K., Qin, Y., Yuan, M.,

467   Huaqun, Y., He, Z., Wu, L., Schuur, E.A.G.G., Tiedje, J.M., ZHOU, J., 2015. Shifts of tundra

468   bacterial and archaeal communities along a permafrost thaw gradient in Alaska. Mol. Ecol.

469   24, 222–234. https://doi.org/10.1111/mec.13015

470 Elberling, B., Michelsen, A., Schädel, C., Schuur, E.A.G., Christiansen, H.H., Berg, L., Tamstorf,

471   M.P., Sigsgaard, C., 2013. Long-term CO2 production following permafrost thaw. Nat. Clim.

472   Chang. 3, 890–894. https://doi.org/10.1038/nclimate1955

473 Fierer, N., Bradford, M.A., Jackson, R.B., 2007. Toward an ecological classification of soil

474   bacteria. Ecology 88, 1354–1364. https://doi.org/10.1890/05-1839

475 Frank-Fahle, B.A., Yergeau, É., Greer, C.W., Lantuit, H., Wagner, D., 2014. Microbial functional

476   potential and community composition in permafrost-affected soils of the NW Canadian

477   Arctic. PLoS One 9. https://doi.org/10.1371/journal.pone.0084761

478 Ganzert, L., Bajerski, F., Wagner, D., 2014. Bacterial community composition and diversity of

479   five different permafrost-affected soils of Northeast Greenland. FEMS Microbiol. Ecol. 89,

480   426–441. https://doi.org/10.1111/1574-6941.12352

26

481 Geisen, S., Hu, S., dela Cruz, T.E.E., Veen, G.F. (Ciska., 2021. Protists as catalyzers of microbial

482   litter breakdown and carbon cycling at different temperature regimes. ISME J. 15, 618–

483   621. https://doi.org/10.1038/s41396-020-00792-y

484 Geisen, S., Tveit, A.T., Clark, I.M., Richter, A., Svenning, M.M., Bonkowski, M., Urich, T., 2015.

485   Metatranscriptomic census of active protists in soils. ISME J. 9, 2178–2190.

486   https://doi.org/10.1038/ismej.2015.30

487 Gittel, A., Bárta, J., Kohoutová, I., Mikutta, R., Owens, S., Gilbert, J., Schnecker, J., Wild, B.,

488   Hannisdal, B., Maerz, J., Lashchinskiy, N., Čapek, P., Šantrůčková, H., Gentsch, N.,

489   Shibistova, O., Guggenberger, G., Richter, A., Torsvik, V.L., Schleper, C., Urich, T.,

490   Kohoutova, I., 2014a. Distinct microbial communities associated with buried soils in the

491   siberian tundra. ISME J. 8, 841–853. https://doi.org/10.1038/ismej.2013.219

492 Gittel, A., Bárta, J., Kohoutová, I., Schnecker, J., Wild, B., Čapek, P., Kaiser, C., Torsvik, V.L.,

493   Richter, A., Schleper, C., Urich, T., Basiliko, N., 2014b. Site- and horizon-specific patterns of

494   microbial community structure and enzyme activities in permafrost-affected soils of

495   Greenland. Front. Microbiol. 5, 1–14. https://doi.org/10.3389/fmicb.2014.00541

496 Griffiths, B.S., Philippot, L., 2013. Insights into the resistance and resilience of the soil microbial

497   community. FEMS Microbiol. Rev. 37, 112–129. https://doi.org/10.1111/j.1574-

498   6976.2012.00343.x

499 He, S., Tominski, C., Kappler, A., Behrens, S., Roden, E.E., 2016. Metagenomic analyses of the

500   autotrophic Fe(II)-oxidizing, nitrate-reducing enrichment culture KS. Appl. Environ.

501   Microbiol. 82, 2656–2668. https://doi.org/10.1128/AEM.03493-15

502 Ho, A., Di Lonardo, D.P., Bodelier, P.L.E., 2017. Revisiting life strategy concepts in environmental

27

503   microbial ecology. FEMS Microbiol. Ecol. 93, 1–14. https://doi.org/10.1093/femsec/fix006

504   Hugelius, G., Strauss, J., Zubrzycki, S., Harden, J.W., Schuur, E.A.G.G., Ping, C.L., Schirrmeister,

505   L., Grosse, G., Michaelson, G.J., Koven, C.D., O'Donnell, J.A., Elberling, B., Mishra, U.,

506   Camill, P., Yu, Z., Palmtag, J., Kuhry, P., 2014. Estimated stocks of circumpolar permafrost

507   carbon with quantified uncertainty ranges and identified data gaps. Biogeosciences 6573–

508   6593. https://doi.org/10.5194/bg-11-6573-2014

509   Hultman, J., Waldrop, M.P., Mackelprang, R., David, M.M., McFarland, J., Blazewicz, S.J.,

510   Harden, J., Turetsky, M.R., McGuire, A.D., Shah, M.B., Verberkmoes, N.C., Lee, L.H.,

511   Mavrommatis, K., Jansson, J.K., 2015. Multi-omics of permafrost, active layer and

512   thermokarst bog soil microbiomes. Nature 521, 208–212.

513   https://doi.org/10.1038/nature14238

514   Huntley, S., Hamann, N., Wegener-Feldbrügge, S., Treuner-Lange, A., Kube, M., Reinhardt, R.,

515   Klages, S., Müller, R., Ronning, C.M., Nierman, W.C., Søgaard-Andersen, L., 2011.

516   Comparative genomic analysis of fruiting body formation in myxococcales. Mol. Biol. Evol.

517   28, 1083–1097. https://doi.org/10.1093/molbev/msq292

518   Hurst, C.J., 2019. Understanding Terrestrial Microbial Communities, Volume 6. ed, Advances in

519   Environmental Microbiology. Springer, Berlin Heidelberg. https://doi.org/10.1007/978-3-

520   10777-2

521   Inglese, C.N., Christiansen, C.T., Lamhonwah, D., Moniz, K., Montross, S.N., Lamoureux, S.,

522   Lafrenière, M., Grogan, P., Walker, V.K., 2018. Examination of Soil Microbial Communities

523   after Permafrost Thaw Subsequent to an Active Layer Detachment in the High Arctic.

524   Arctic, Antarct. Alp. Res. 49, 455–472. https://doi.org/10.1657/AAAR0016-066

525   IPCC, 2021. Climate Change 2021: The Physical Science Basis, Intergovernmental Panel on

526   Climate Change (IPCC).

527   Johnson, S.S., Hebsgaard, M.B., Christensen, T.R., Mastepanov, M., Nielsen, R., Munch, K.,

528   Brand, T., Gilbert, M.T.P., Zuber, M.T., Bunce, M., Rønn, R., Gilichincksy, D., Froese, D.,

529   Willerslev, E., 2007. Ancient bacteria show evidence of DNA repair. PNAS 105, 10631–

530   10631. https://doi.org/10.1073/pnas.0710637105

531   Keuper, F., Wild, B., Kummu, M., Beer, C., Blume-Werry, G., Fontaine, S., Gavazov, K., Gentsch,

532   N., Guggenberger, G., Hugelius, G., Jalava, M., Koven, C., Krab, E.J., Kuhry, P., Monteux, S.,

533   Richter, A., Shahzad, T., Weedon, J.T., Dorrepaal, E., 2020. Carbon loss from northern

534   circumpolar permafrost soils amplified by rhizosphere priming. Nat. Geosci. 13, 560–565.

535   https://doi.org/10.1038/s41561-020-0607-0

536   Kopylova, E., Noé, L., Touzet, H., 2012. Sequence analysis SortMeRNA: fast and accurate

537   filtering of ribosomal RNAs in metatranscriptomic data. Bioinformatics 28, 3211–3217.

538   https://doi.org/10.1093/bioinformatics/bts611

539   Lanzén, A., Jørgensen, S.L., Huson, D.H., Gorfer, M., Grindhaug, S.H., Jonassen, I., Øvreås, L.,

540   Urich, T., 2012. CREST – Classification Resources for Environmental Sequence Tags. PLoS

541   One 7. https://doi.org/10.1371/journal.pone.0049334

542   Lennon, J.T., Jones, S.E., 2011. Microbial seed banks: The ecological and evolutionary

543   implications of dormancy. Nat. Rev. Microbiol. 9, 119–130.

544   https://doi.org/10.1038/nrmicro2504

545   Malard, L.A., Pearce, D.A., 2018. Microbial diversity and biogeography in Arctic soils. Environ.

546   Microbiol. Rep. 10, 611–625. https://doi.org/10.1111/1758-2229.12680

547   McMurdie, P.J., Holmes, S., 2013. phyloseq : An R Package for Reproducible Interactive Analysis

548   and Graphics of Microbiome Census Data. PLoS One 8.

549   https://doi.org/10.1371/journal.pone.0061217

550   Metcalfe, D.B., Hermans, T.D.G., Ahlstrand, J., Becker, M., Berggren, M., Björk, R.G., Björkman,

551   M.P., Blok, D., Chaudhary, N., Chisholm, C., Classen, A.T., Hasselquist, N.J., Jonsson, M.,

552   Kristensen, J.A., Kumordzi, B.B., Lee, H., Mayor, J.R., Prevéy, J., Pantazatou, K., Rousk, J.,

553   Sponseller, R.A., Sundqvist, M.K., Tang, J., Uddling, J., 2018. Patchy field sampling biases

554   understanding of climate change impacts across the Arctic. Nat. Ecol. Evol. 2.

555   https://doi.org/10.1038/s41559-018-0612-5

556   Mondini, A., Anwar, M.Z., Ellegaard-jensen, L., Lavin, P., Jacobsen, C.S., Purcarea, C., 2022. Heat

557   Shock Response of the Active Microbiome From Perennial Cave Ice. Front. Microbiol. 12,

558   1–14. https://doi.org/10.3389/fmicb.2021.809076

559   Monteux, S., Keuper, F., Fontaine, S., Gavazov, K., Hallin, S., Juhanson, J., Krab, E.J., Revaillot, S.,

560   Verbruggen, E., Walz, J., Weedon, J.T., Dorrepaal, E., 2020. Carbon and nitrogen cycling in

561   Yedoma permafrost controlled by microbial functional limitations. Nat. Geosci. 13, 794–

562   798. https://doi.org/10.1038/s41561-020-00662-4

563   Monteux, S., Weedon, J.T., Blume-Werry, G., Gavazov, K., Jassey, V.E.J., Johansson, M., Keuper,

564   F., Olid, C., Dorrepaal, E., Gavazov, G.B.K., Blume-Werry, G., Gavazov, K., Jassey, V.E.J.,

565   Johansson, M., Keuper, F., Olid, C., Dorrepaal, E., 2018. Long-term in situ permafrost thaw

566   effects on bacterial communities and potential aerobic respiration. ISME J. 12, 2129–2141.

567   https://doi.org/10.1038/s41396-018-0176-z

568   Müller, O., Bang-Andreasen, T., White, R.A., Elberling, B., Taş, N., Kneafsey, T., Jansson, J.K.,

30

569   Øvreås, L., Allen, R., Iii, W., Elberling, B., Tas, N., Kneafsey, T., Jansson, J.K., Øvreås, L.,

570   White, R.A., Elberling, B., Taş, N., Kneafsey, T., Jansson, J.K., Øvreås, L., Allen, R., Iii, W.,

571   Elberling, B., Tas, N., Kneafsey, T., Jansson, J.K., Øvreås, L., 2018. Disentangling the

572   complexity of permafrost soil by using high resolution profiling of microbial community

573   composition, key functions and respiration rates. Environ. Microbiol. 20, 4328–4342.

574   https://doi.org/10.1111/1462-2920.14348

575   Nannipieri, P., Ascher, J., Ceccherini, M.T., Landi, L., Pietramellara, G., Renella, G., 2017.

576   Microbial diversity and soil functions. Eur. J. Soil Sci. 68, 12–26.

577   https://doi.org/10.1111/ejss.4_12398

578   Naylor, D., McClure, R., Jansson, J., 2022. Trends in Microbial Community Composition and

579   Function by Soil Depth. MDPI Microorg. 10.

580   Oksanen, J., Blanchet, F.G., Friendly, M., Kindt, R., Legendre, P., McGlinn, D., Minchin, P.R.,

581   O'Hara, R.B., Simpson, G.L., Solymos, P., Stevens, M.H.H., Szoecs, E., Wagner, H., 2020.

582   vegan: Community Ecology Package. R package version 2.5-7.

583   Parmentier, F.-J.W., Christensen, T.R., Rysgaard, S., Bendtsen, J., Glud, R.N., Else, B., Huissteden,

584   J. Van, Sachs, T., Vonk, J.E., Sejr, M.K., 2017. A synthesis of the arctic terrestrial and marine

585   carbon cycles under pressure from a dwindling cryosphere. Ambio 46, 53–69.

586   https://doi.org/10.1007/s13280-016-0872-8

587   Petters, S., Groß, V., Söllinger, A., Pichler, M., Reinhard, A., Bengtsson, M.M., Urich, T., 2021.

588   The soil microbial food web revisited: Predatory myxobacteria as keystone taxa? ISME J.

589   15, 2665–2675. https://doi.org/10.1038/s41396-021-00958-2

590   Quast, C., Pruesse, E., Yilmaz, P., Gerken, J., Schweer, T., Glo, F.O., Yarza, P., 2013. The SILVA

31

591 ribosomal RNA gene database project : improved data processing and web-based tools 41,

592 590–596. https://doi.org/10.1093/nar/gks1219

593 Rønn, R., Vestergård, M., Ekelund, F., 2012. Interactions between bacteria, protozoa and

594 nematodes in soil. Acta Protozool. 51, 223–235.

595 https://doi.org/10.4467/16890027AP.12.018.0764

596 Scheel, M., Zervas, A., Jacobsen, C.S., Christensen, T.R., 2022. Microbial Community Changes in

597 26,500-Year-Old Thawing Permafrost. Front. Microbiol. 13, 1–14.

598 https://doi.org/10.3389/fmicb.2022.787146

599 Scheller, J.H., Mastepanov, M., Christiansen, H.H., Christensen, T.R., 2021. Methane in

600 Zackenberg Valley, NE Greenland: multidecadal growing season fluxes of a high-Arctic

601 tundra. Biogeosciences 18, 6093–6114. https://doi.org/10.5194/bg-18-6093-2021

602 Schostag, M., Priemé, A., Jacquiod, S., Russel, J., Ekelund, F., Jacobsen, C.S., 2019. Bacterial and

603 protozoan dynamics upon thawing and freezing of an active layer permafrost soil. ISME J.

604 13, 1345–1359. https://doi.org/10.1038/s41396-019-0351-x

605 Schostag, M.D., Albers, C.N., Jacobsen, C.S., Priemé, A., 2020. Low Turnover of Soil Bacterial

606 rRNA at Low Temperatures. Front. Microbiol. 11, 1–5.

607 https://doi.org/10.3389/fmicb.2020.00962

608 Shade, A., Jones, S.E., Gregory Caporaso, J., Handelsman, J., Knight, R., Fierer, N., Gilbert, J.A.,

609 2014. Conditionally rare taxa disproportionately contribute to temporal changes in

610 microbial diversity. MBio 5. https://doi.org/10.1128/mBio.01371-14

611 Shade, A., Peter, H., Allison, S.D., Baho, D.L., Berga, M., Bürgmann, H., Huber, D.H.,

612 Langenheder, S., Lennon, J.T., Martiny, J.B.H., Matulich, K.L., Schmidt, T.M., Handelsman,

613   J., 2012. Fundamentals of microbial community resistance and resilience. Front. Microbiol.

614   3, 1–19. https://doi.org/10.3389/fmicb.2012.00417

615 Shatilovich, A. V., Shmakova, L.A., Mylnikov, A.P., Gilichinsky, D.A., 2009. Ancient Protozoa

616   Isolated from Permafrost. Permafr. Soils 97–115. https://doi.org/10.1007/978-3-540-

617   69371-0_8

618 Tarnocai, C., Canadell, J.G., Schuur, E.A.G.G., Kuhry, P., Mazhitova, G., Zimov, S., Tarnocai, C.,

619   Canadell, J.G., Schuur, E.A.G.G., Kuhry, P., Mazhitova, G., Zimov, S., Tamocai, C., Canadell,

620   J.G., Schuur, E.A.G.G., Kuhry, P., Mazhitova, G., Zimov, S., Tarnocai, C., Canadell, J.G.,

621   Schuur, E.A.G.G., Kuhry, P., Mazhitova, G., Zimov, S., Tamocai, C., Canadell, J.G., Schuur,

622   E.A.G.G., Kuhry, P., Mazhitova, G., Zimov, S., 2009. Soil organic carbon pools in the

623   northern circumpolar permafrost region. Global Biogeochem. Cycles 23, 1–11.

624   https://doi.org/10.1029/2008GB003327

625 Thakur, M.P., Geisen, S., 2019. Trophic Regulations of the Soil Microbiome. Trends Microbiol.

626   27, 771–780. https://doi.org/10.1016/j.tim.2019.04.008

627 Tripathi, B.M., Kim, M., Kim, Y., Byun, E., Yang, J.W., Ahn, J., Lee, Y.K., 2018. Variations in

628   bacterial and archaeal communities along depth profiles of Alaskan soil cores. Nat. Sci.

629   Reports 8, 1–11. https://doi.org/10.1038/s41598-017-18777-x

630 Turetsky, M., Abbott, B., Jones, M., Walter Anthony, K.M., Olefeldt, D., Schuur, E.A.G., Grosse,

631   G., Kuhry, P., Hugelius, G., Koven, C.D., Lawrence, D.M., Gibson, C., Sannel, A., McGuire,

632   A.D., 2020. Carbon release through abrupt permafrost thaw. Nat. Geosci. 13, 138–143.

633   https://doi.org/10.1038/s41561-019-0526-0

634 Tveit, A.T., Schwacke, R., Svenning, M.M., Urich, T., 2013. Organic carbon transformations in

635   high-Arctic peat soils : key functions and microorganisms. ISME J. 7, 299–311.

636   https://doi.org/10.1038/ismej.2012.99

637 Tveit, A.T., Urich, T., Frenzel, P., Marianne, M., Tveit, A.T., Urich, T., Frenzel, P., Svenning, M.M.,

638   2015. Metabolic and trophic interactions modulate methane production by Arctic peat

639   microbiota in response to warming. Proc. Natl. Acad. Sci. U. S. A. 112, E2507–E2516.

640   https://doi.org/10.1073/pnas.1420797112

641 Urich, T., Lanzén, A., Qi, J., Huson, D.H., Schleper, C., Schuster, S.C., Urich, T., Lanze, A., 2008.

642   Simultaneous assessment of soil microbial community structure and function through

643   analysis of the meta-transcriptome. PLoS One 3.

644   https://doi.org/10.1371/journal.pone.0002527

645 Xue, Y., Lanzén, A., Jonassen, I., 2020. Sequence analysis Reconstructing ribosomal genes from

646   large scale total RNA meta-transcriptomic data. Bioinformatics 36, 3365–3371.

647   https://doi.org/10.1093/bioinformatics/btaa177

648 Zhang, L., Lueders, T., 2017. Micropredator niche differentiation between bulk soil and

649   rhizosphere of an agricultural soil depends on bacterial prey. FEMS Microbiol. Ecol. 93, 1–

650   11. https://doi.org/10.1093/femsec/fix103

651

9. Figure descriptions

652

653 Figure 1 (A) Sampling site Zackenberg in Northeast Greenland, credit: Google Earth. (B)

654 Sampling site in 2018 after initial permafrost collapse. (C) Soil profile from the surface until still

655 frozen depth at 90 cm during sampling in 2020. (D) Scheme of abrupt permafrost thaw

656 (indicated with blue arrows), depicting the soil profile until the permafrost (PF) layer at 90–100

657 cm depth from the moment of collapse in 2018 with visible ice lens below long-term active

658 layer (AL) to the formation of transition zones (TZ, = thawed permafrost).
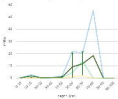
659 Figure 2 (A) Dry weight (DW) normalised RNA:DNA ratio per gram sample was indicated for

660 each extraction triplicate and the resulting mean. The mean co-extracted DNA (B) and RNA (C)

661 content in ng/µl per g DW per depth as measured using TapeStation assays. Whiskers indicate

662 the standard deviation among the extraction triplicates.

663 Figure 3 Bar plot indicating the relative mean abundance per depth. The brackets indicate the

664 next lower taxonomic level of (A) prokaryotic classes with < 1% of total community relative

665 abundance, (B) bacterial predator families, (C) eukaryotic kingdoms, and (D) protozoan phyla.

666 Figure 4 Shannon alpha diversity for prokaryotes (A), bacterial predators (B), and protozoa (C)

667 given as boxplots with whiskers indicating standard deviation, shapes indicating the layer of

668 samples (AL = active layer; TZ1, TZ2 = transition zone 1 and 2; PF = permafrost), while colours

669 indicate age categories (AY = young age in blue; AM = medium age in green; AO = old age in red,

670 see also Table 1).

35

671   Figure 5 Principal component analysis (PCoA) ordination plots performed on relative rRNA

672   contig abundances per sample for (A) prokaryotes, bacterial predators (B), eukaryotes (C), and

673   protozoa (D). Environmental parameters here are given as layer (active layer AL, transition zone

674   1 TZ1 and 2 TZ2, and permafrost PF) as well as age with young soils (AY), 2 634–3 770-year-old

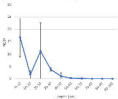675   soil of medium age (AM), and old material (AO) of up to 22 100–26 500 years age.

A   B   C